Constrained control of coexisting attractors in impact oscillator with delay

Mohsen Lalehparvar, Vahid Vaziri and Sumeet S. Aphale

Centre for Applied Dynamics Research, School of Engineering, University of Aberdeen, Old Aberdeen, Aberdeen, AB24 3UE, Scotland, UK.

*Corresponding author(s). E-mail(s): vahid.vaziri@abdn.ac.uk;

Abstract

The coexistence of attractors is a characteristic of a range of nonlinear systems that results in systems exhibiting different dynamics for varying initial conditions with invariant system parameters. This characteristic often provides an effective means to jump between different behaviours by employing control methods. However, control signals are influenced by delay and constraint, which affect controllers' performance. In this paper, we investigate the effects of actuator and memory delay, start time and actuator constraints on the performance of the time-delayed feedback (TDF) control scheme enabling the switching between coexisting attractors of the impact oscillator. Looking at two potential applications, we focused on two case studies with two desired stable orbits: Case 1: Non-impacting attractor and Case 2: High amplitude attractor. In both case studies, the effects of the actuator and memory delay in the control signal are investigated. Then, within a meaningful range of delay, their effects on the controller performance are predicted and compared. One notable observation is that by increasing the delay, settling time follows similar patterns in two case studies, experiencing a decrease followed by an increase and then failure of the controller to jump between the targeted coexisting attractors. Furthermore, the effects of the start time and the actuator constraints (force limit) on the controllers' performances in these case studies are also investigated.

Keywords: Time delay, Constraint control, Time-delayed feedback control, Impact oscillator

1 Introduction

One of the main characteristics of nonlinear systems is the coexisting attractors (or multistability), which refers to the coexistence of several attractors (or equilibrium states) for a fixed set of parameters in a system [1, 2]. Multistability makes switching between two coexisting attractors possible to get the desired response suitable for the chosen application. For example, chaotic and non-chaotic responses might coexist in a system [3]. For some applications, chaotic behaviour might be desired as an intermediate dynamical regime [4]. On the contrary, chaotic behaviour might be undesired in some applications, and multistability might be used to drive the system out of chaos [5]. Exploiting multistability can also be used to drive the system to the desired response with only small perturbations [5, 6].

Exchanging the impacting and non-impacting coexisting attractors can be performed depending on the application. It might be desired to avoid impact to exchange to a non-impacting attractor to avoid imperfections during the machining process [7, 8]. In Jeffcott rotors, the impact of the rotor and the snubber ring results in the degradation of the system, and it is desired to be avoided. To this purpose, the exchange between impacting to non-impacting attractor jumps the system from the impacting to the non-impacting attractor [9, 10]. Similarly, the impact should be avoided in the railway wheelset to increase the system's lifetime. This can be done by the exchange to a non-impacting attractor in double grazing bifurcation [11]. To the same purpose, impacting and non-impacting multistability can be exploited to avoid impact and impact-caused damages in elastic beams [12, 13]. The impact of ships with icebergs due to the roll motion can also be controlled in grazing point [14–16]. Jumping from impacting as one stability status to a coexisting non-impacting one with different actuation behaviour [17, 18] is another example of such an attractor exchange.

On the contrary, impacting attractors might be desired for some nonlinear systems. For example, for energy generation, the impacts might increase the domain of oscillations and consequently the energy output [19]. Impacting can also be used in vibro-impacting energy harvesters where this nonlinear phenomenon can be used to increase the amplitudes of higher-order vibration modes, hence, more energy output [20–22]. Bistability in low-energy interwell vibrations and high-energy snap-through in some energy harvesters provides a means by which energy harvesting performance could be improved [23]. Resonance Enhanced Drilling (RED) is another application at which the impacting attractors are desired[24–26]. In this method, the high frequency, low amplitude impacts create a controllable propagating fracture zone at the rock face.

Active control methods should be applied to achieve the exchange between coexisting attractors, utilising actuators [27, 28]. However, actuators such

as electrical motors, hydraulic and pneumatic valves do not typically have instantaneous responses in real-world engineering systems. Hence, their dynamics usually involve two key limitations: (i) delay and (ii) input/output constraints (actuator saturation) [29, 30]. Recent attempts to overcome actuator delay have shown limited success [31, 32]. It has also emerged that the effect of the simultaneous existence of both limitations (delay and constraint) cannot be ignored, as they would make the control systems inefficient and occasionally unstable [33, 34].

The main idea of this work is to examine the effects of delay and actuator constraints while exchanging between coexisting attractors. In this regard, two case studies with two desired stable orbits are considered; Case 1: Non-impacting attractor and Case 2: High amplitude attractor. The impact oscillator can exhibit many different attractors, which is a suitable platform for such an analysis. The mass-excited impact oscillator developed in the Centre for Applied Dynamics Research (CADR) [35, 36] is then selected so the experimentally validated model [28] can be employed for this analysis.

The paper is organized as follows. Section 2 presents the mathematical modelling and dynamics of the open loop system. The first case study (Case 1) and relevant control method to achieve the non-impacting attractor in the presence of the delay and actuator constraints are presented in Section 3. The second case study (Case 2) and the additional intermediate control strategy to achieve a higher amplitude attractor are introduced in Section 4. Section 5 concludes this paper.

2 Mathematical modelling and system dynamics

The mass-excited impact oscillator is composed of a mass hung by two leaf springs excited by a coil, as shown in Fig. 1. The system is linear to the point that the oscillation amplitude becomes greater than the initial gap, g. Hereafter, the impact between the mass and the impacting beam makes the system nonlinear. The equation of motion governing the system is as follows:

$$\ddot{X} = -\frac{k_1}{m}\ X - \frac{k_2}{m}(X-g)H(X-g) - \frac{c}{m}\dot{X} + \frac{F_{coil}}{m}, \tag{1}$$

where X is the displacement, $H(.)$ is the Heaviside's step function, the dot represents the time derivative, and F_{coil} is the force provided by the coil. F_{coil} is a sum of the harmonic excitation applied to the system $F_{exc} = aI_0 sin(\omega t)$, where I_0 is the excitation current amplitude, and actuation force $F_{act} = aI_{act}$ which is dictated by the control method. Note that in the open loop system, I_{act} is zero. The system parameters are fully reported in Table 1. Note that the model is based on the experiments done in CADR and reported in [35]. In section 3.3 of the mentioned paper, the coefficient of damping and stiffness

Table 1: System parameters.

Symbol	Value	Unit
m	1.325	kg
k_1	4331	N/m
k_2	87125	N/m
c	0.27	kg/s^2
g	0.74	mm
a	0.799	N/A
I_0	1.45	A

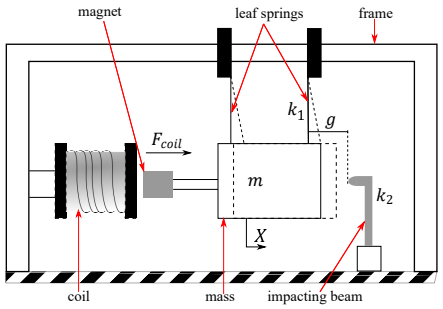

Figure 1: Schematic of mass-excited impact oscillator.

have been obtained through free vibration tests.

Since nonlinear systems dynamics are determined by their initial conditions, the basin of attraction is obtained for the excitation frequency of 6.8 Hz, Fig. 2, (c). This basin of attraction is calculated in a range displacement of [-2 2] mm and velocity of [-2 2] mm/s which illustrates the coexistence of p1 and p2 attractors. Note that the basin of attraction is obtained coarsely by steps of 0.1 mm and 0.1 mm/s for displacement and velocity, respectively. These step sizes were accurate enough to capture the coexistence of p1 and p2 along with their corresponding initial conditions. However, this basin of attraction is not detailed to cover all possible responses and patterns in the given frequency.

To gain more insight into the system, using the information from the basin of attraction at 6.8 Hz, the bifurcation diagram is obtained, which illustrates the behaviour of the system in a range of 6.6 Hz to 8.6 Hz, Fig. 2, (d). Note this frequency range is chosen following the experimentally obtained diagram in [28]. As shown in Fig. 2, (d), The system responses include period one (p1), period two (p2), period three (p3), period four (p4), and higher period and chaotic responses (else). Since the maximum amplitude contrast (maximum-minimum) of system response is desired in some applications, another bifurcation diagram illustrating amplitude contrast versus excitation frequency is also obtained, Fig. 2, (b). Note that as shown in Fig. 2, (b), the amplitude in 6.8 Hz indicates a difference of around 0.7 mm between p1 and p2 responses.

As discussed earlier, switching from an undesired attractor to the desired one is required for many applications. In the following sections, we present two case studies and discuss the effect of the delay and actuator constraints on the settling time of the two desired attractors; (i) non-impacting attractor and (ii) high amplitude attractor.

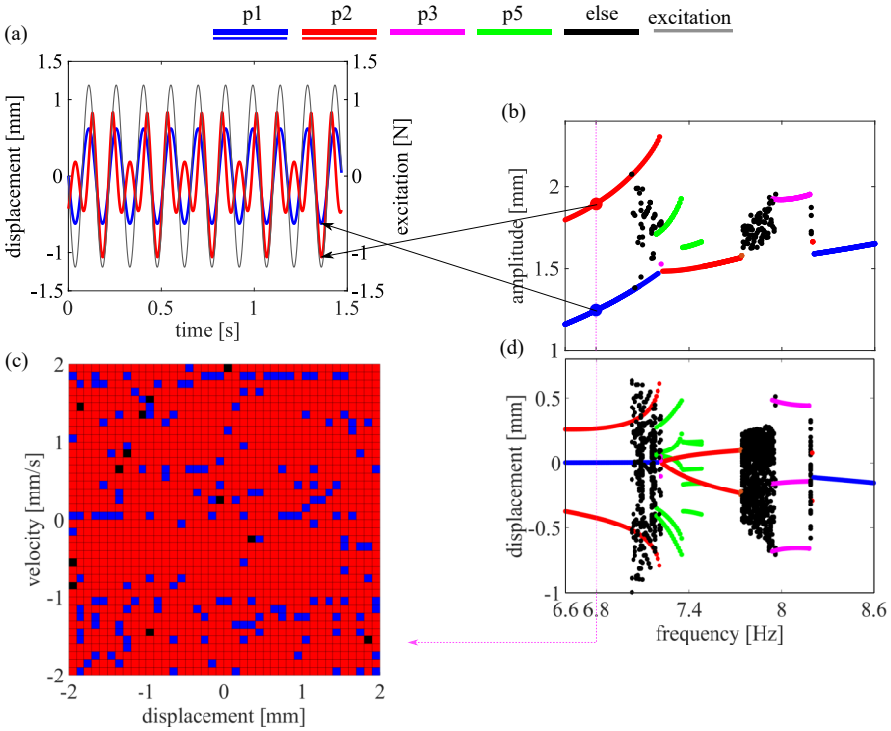

Figure 2: Dynamics analysis of the system. (a) Ten periods of the time history of the coexisting p1 and p2 responses at the excitation frequency of 6.8 Hz. (b) Non-standard bifurcation diagram; the amplitude contrast of system response versus excitation frequency. (c) Basin of attraction at 6.8 Hz. (d) Standard bifurcation diagram.

3 First case study: Switching to non-impacting attractor

Impacts might result in damage or degradation in mechanical systems. As a result, it is largely desired to avoid impact. This can be done by exchanging attractors when an impacting attractor coexists with a non-impacting one. In the first case study, we investigate this goal in the impact oscillator. As the only source of nonlinearity in the impact oscillator is the impact, the only non-impacting orbit must be p1 (linear response). Therefore the goal of this case study is to switch other attractors to p1. Time-delayed feedback (TDF) control is employed for this purpose. TDF is a simple-design controller which does not require an external reference signal, hence, does not require substantial prior knowledge of the system and is suitable for experimental applications [37]. As shown in the block diagram of the system, Fig. 3, to form the control signal, a weighted comparison of the current $Y(t)$ and delayed $Y(t-\tau_s)$ states of the

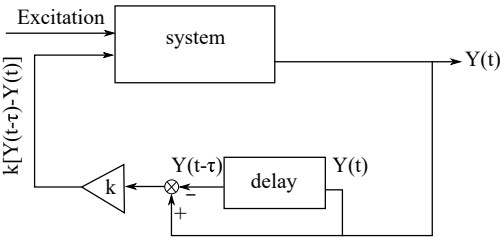

Figure 3: Generalised form of the externally excited system with the TDF control scheme.

system is used. Note in the impact oscillator $Y(t) = [x(t), \dot{x}(t)]'$. Following the work presented in [28], we can calculate the control signal as follows:

$$aI_{act} = \begin{bmatrix} K_p & K_v \end{bmatrix} \begin{bmatrix} x(t-\tau) - x(t) \\ \dot{x}(t-\tau) - \dot{x}(t) \end{bmatrix}, \tag{2}$$

where K_p and K_v are the control gains and τ is the controller time delay.

By setting $\tau = T$, the TDF controller successfully performs the exchange from p2 to p1 in about 3 S (Fig. 4), and the control signal converges to zero when the system fully settles in p1. In an ideal system, there are not any delay or actuator constraints. However, a delay exists in real-world systems. Also, due to the physical limits, actuators are imperfect and are subject to constraint [29]. Actuator delay is caused by latency in the actuation parts of the system. In contrast, memory delay causes by the latency in the data storage and reading process while obtaining the delayed states. These two types of delay can be added to the TDF signal and formulated as follows:

$$aI_{act1}(t + \tau_s) = \begin{bmatrix} K_p & K_v \end{bmatrix} \begin{bmatrix} x(t-\tau) - x(t) \\ \dot{x}(t-\tau) - \dot{x}(t) \end{bmatrix}, \tag{3}$$

$$aI_{act2}(t) = \begin{bmatrix} K_p & K_v \end{bmatrix} \begin{bmatrix} x(t-\tau-\tau_s) - x(t) \\ \dot{x}(t-\tau-\tau_s) - \dot{x}(t) \end{bmatrix}, \tag{4}$$

where I_{act1} and I_{act2} are actuation currents in the presence of the actuator and memory delay, respectively and τ_s is the system's delay.

To assess the effect of delay on the controller's performance, a delay up to 0.2 of the period ($0.2T$ where $T = 0.1471$s) is applied to the system in two different forms, actuator delay and memory delay, Fig. 5, (e). By increasing the delay, settling time undergoes a decrease to about $8T$ and $6T$ for actuator and memory delay, respectively. After these minimums, settling time increases to around $22T$ for both cases, after which the controller fails to stabilize the system in p1. Time histories and control signals of the middle range and maximum range of delay are presented in Fig. 5,(a), (c), (h) and (j).

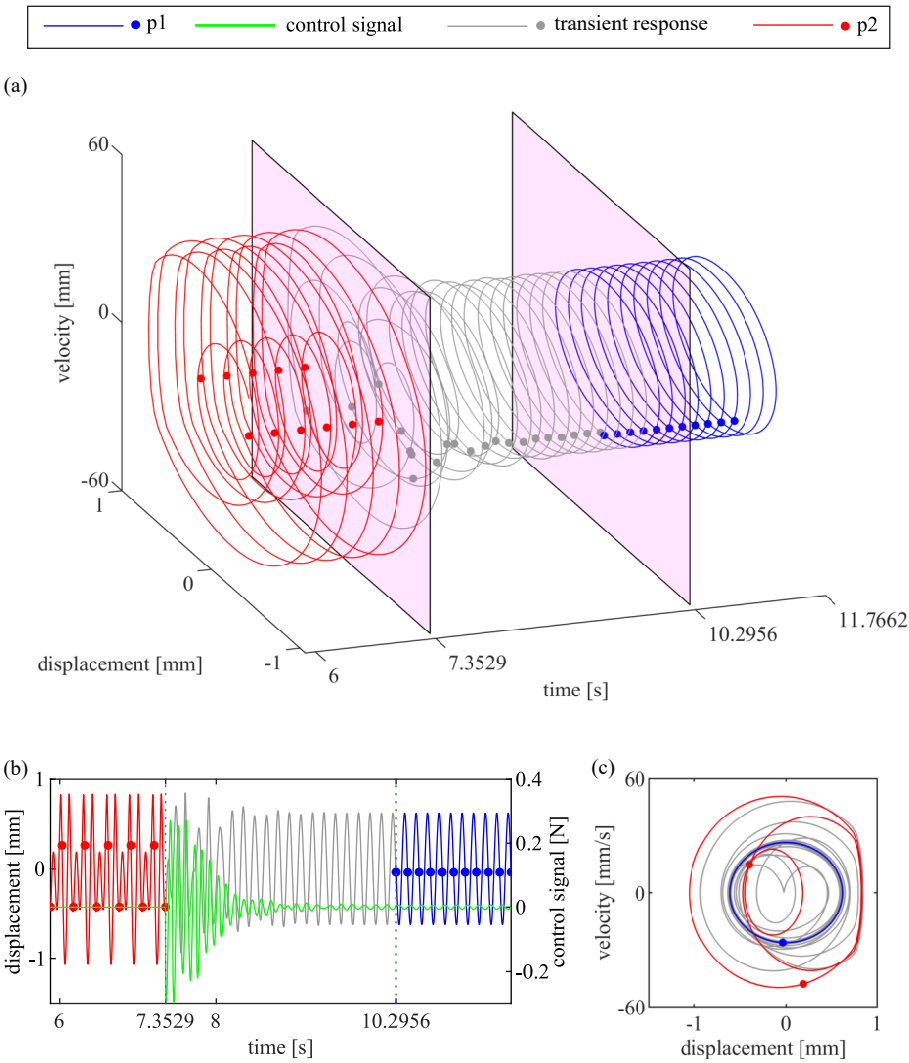

Figure 4: Exchange of p2 to p1 in the system without any delay or actuator constraints. 3D (a) and 2D (b) time histories of the system response illustrated ten periods of excitation before and after the exchange and the transient time. Note that the control signal is plotted in green. (c) Phase plane, which indicates a successful transition from p2 to p1.

The system could be at any phase of its response period when the controller takes effect. This phase can be represented by the time that has passed since the start of the period. Here we call it the start time of the controller. The effect of the start time on the settling time, then, is investigated in the range of zero (beginning of the period) to two periods of response, $2T$ (the

end of the period of response, p2). As seen in Fig. 5, (f), by increasing the start time, settling time starts decreasing; however, it undergoes intermittent jumps, which results in the maximum difference of about eight periods of excitation, $8T$. Time histories and control signals of two cases are presented in Fig. 5,(i) and (k).

To evaluate the effects of actuator constraints on the TDF's performance, a force limit, ranging from 0.2 N down to 0.06 N, is applied to the absolute value of the control signal. Owing to the fact that the effect of constraint increases when the absolute value of the force limit decreases, the constraint limit is applied to the system decreasingly. As shown in Fig. 5, (g), by increasing the effect of constraint (decreasing the limit), the settling time of the system increases to the point that the controller fails to perform the exchange. Time histories and control signals of two cases are presented in Fig. 5, (b) and (d).

Fig. 5 demonstrates that when the controller performs the switch between p2 to p1, the settling time of the system can increase by about five times with the presence of a delay. Also, it shows that settling time can increase by about two and half times depending on the start time of the controller and finally, it shows that the settling time can increase by about two times when the limitations on the control signal (force) decrease by 30 times.

4 Second case study: Switching to high amplitude attractor

As shown in the system dynamics Fig. 2, (a) and (b), p2 has a higher amplitude than p1. Hence, when the higher amplitude of oscillation is favourable [20–22] or impacting response is desired [24], switching from p1 to p2 is required. Therefore the aim of the second case study is to switch p1 to p2 in the impact oscillator. However, this exchange is more complex than a p2 to p1 exchange using the TDF controller. The reason is that the controller time delay in p1 is the factor of higher periods. In other words, delay in periods higher than p1 is an integer multiplier of the period of oscillation which is equal to the period of p1. So as long as the system is in p1, the control signal remains zero (even when $\tau = 2T$). To resolve this issue, a two-staged TDF is applied to the system [28]. During the first stage, the controller takes the system out of the basing of attraction of p1 with a non-integer delay ($\tau = 0.5T$ in this case). When the system is out of p1, the controller takes the system to p2 with $\tau = 2T$ in the second stage, Fig. 6.

Since the first stage of the controller only takes the system out of p1, the control time delay can be any non-integer number that produces a control signal to take the system out of p1. Note any integer number of delay results in zero control signal. Hence, it can be something other than, necessarily or

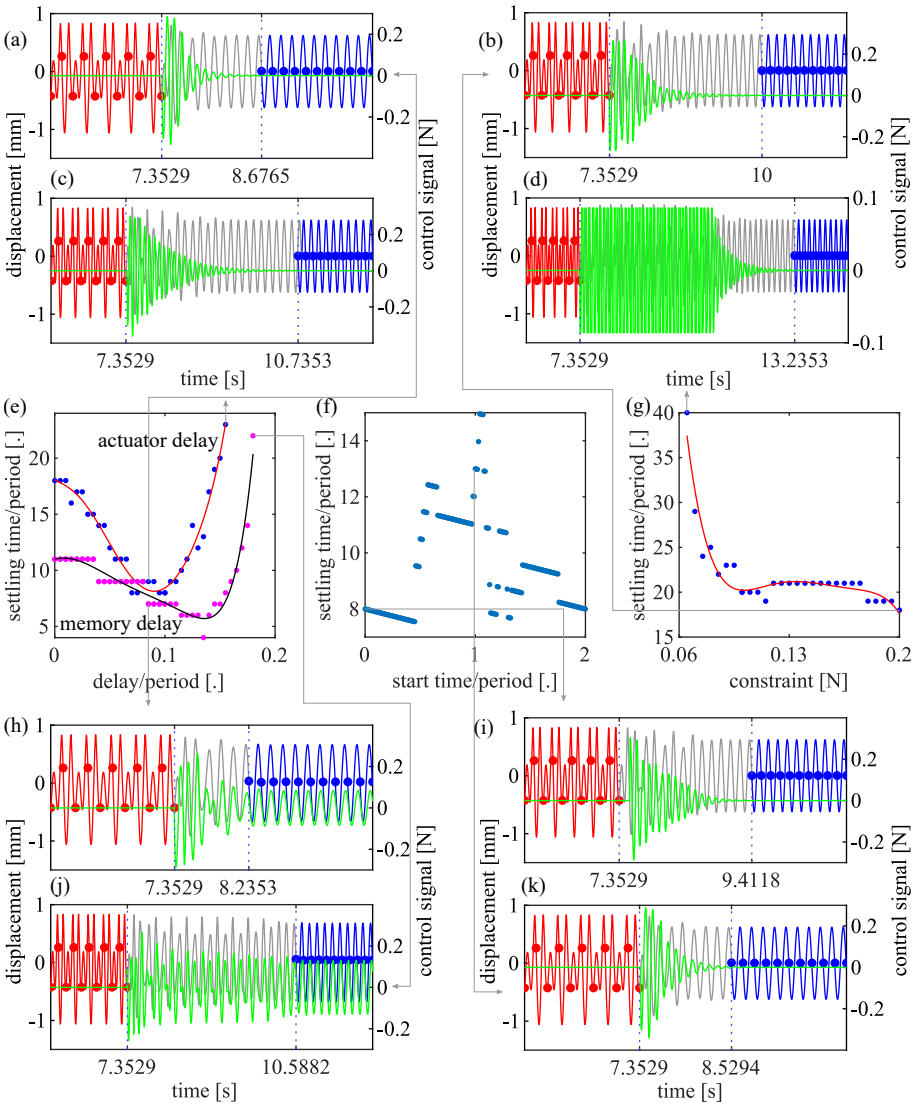

Figure 5: Effects of actuator delay (Eq. 3), memory delay (Eq. 4), the start time of the controller and constraint on the controller's performance in Case 1. (e) Settling time versus delay. (f) Settling time versus start time of the controller. (g) Settling time versus the constraint (limit on the output force). Note that other panels are time histories and control signals of selective cases.

precisely $0.5T$. Therefore the delay and constraint are applied only to the second stage of the control process. Nevertheless, in this case, the system illustrates more sensitivity to delay and constraint. As shown in Fig. 7, (e), by increasing the memory delay, settling time follows more or less the same

pattern as the Case 1, however, in a much smaller range. At around $0.07T$, the settling time is around $390T$, and by increasing the delay more, the controller fails to perform the exchange. Similarly, by increasing the actuator delay, settling time experiences a U-typed graph up to around $0.011T$, after which the controller fails to stabilize the system. It is worth noting that the settling time is obtained by making a comparison of the average of Poincaré sections of the last 200 periods of the response with the corresponding delayed states, taking into account a comparison error of 10^{-6} mm and 10^{-6} mm/s for displacement and velocity, respectively. As shown in Fig. 7,(c), although the controller takes the system nearly to p2 in around 30s, it takes around 67s for the controller to achieve the defined accuracy.

As shown in Fig. 7,(f), by increasing the start time of the controller, the settling time decreases. However, similar to Case 1, it undergoes a few intermittent jumps, which results in the maximum settling time difference equal to around $2T$, which is lower than the Case 1. Hence, the system, in this case, is less sensitive to the time when the controller kicks in.

By increasing the effect of constraint or decreasing the norm of the constraint cap from 0.2 N, the system illustrates an unexpected behaviour, Fig. 7,(g). By decreasing the norm of the force limit up to 0.03 N, the settling time remains constant. However, by a further decrease in the norm up to 0.25 N, settling time experiences a decrease to around $25T$, after which the controller fails to stabilize the system and perform the exchange to p2.

Fig. 7 demonstrates that when the controller performs the switch between p1 to p2, the settling time of the system can increase by about 15% with the presence of a delay. Also, it shows the limitations of the control signal, and the start time of the controller has a minimum influence on the settling time.

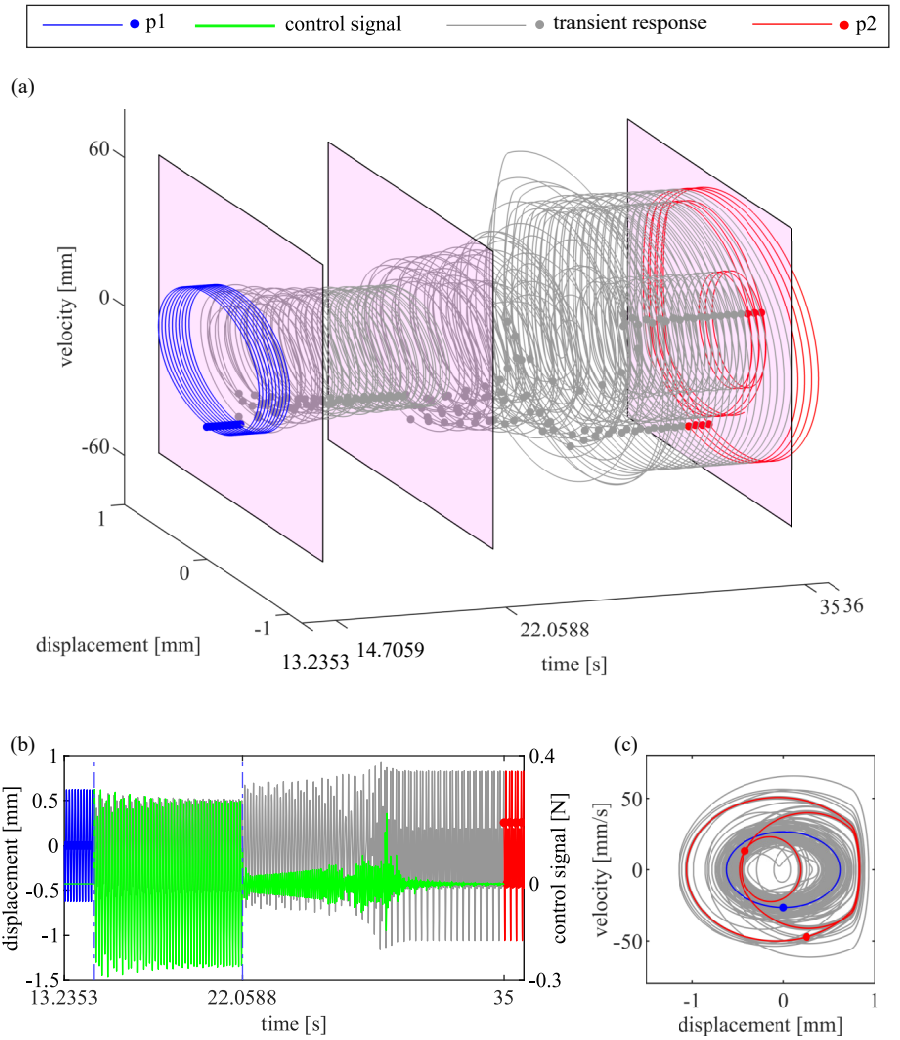

Figure 6: Exchange of p1 to p2 in the system without any delay or actuator constraints. 3D (a) and 2D (b) time histories of the system response illustrated ten periods of excitation before and after the exchange and the transient time. Note that the control signal is plotted in green. (c) Phase plane, which indicates a successful transition from p1 to p2.

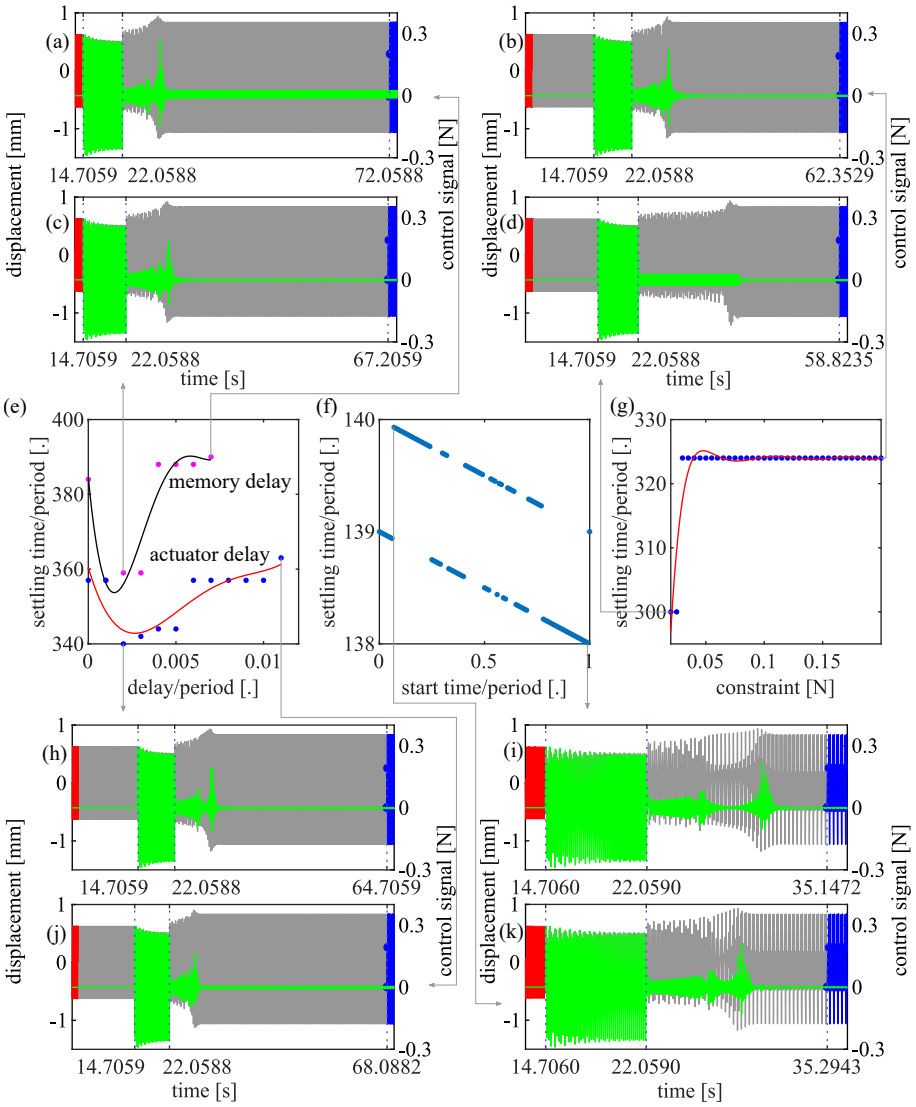

Figure 7: Effects of actuator delay, memory delay, the start time of the controller and constraint on the controller's performance in Case 2. (e) Settling time versus delay. (f) Settling time versus start time of the controller. (g) Settling time versus the constraint. Note that other panels are time histories and control signals of selective cases.

5 Conclusions

The effects of delay, start time, and actuator constraints have been investigated by considering two case studies of desired attractors: Case 1: Non-impacting attractor, and Case 2: High amplitude attractor. The chosen controller is initially employed in the nominal system (without delay) to demonstrate its efficiency. In both case studies, it is seen that an increase in delay results in a decrease in settling time and then an increase, gradually leading to the controller's failure. However, the delay range in which the controller is successful in Case 2 is much less than its corresponding Case 1 (about 19 times). By delaying the start time, settling time in both cases undergoes some falling intervals with intermittent jumps. The maximum difference in the settling time in Case 1 is about four times the one in Case 2, which makes this case more sensitive to when the controller is engaged. Finally, the system indicates two opposing behaviours by increasing the constraint effects (decreasing the force limit). By decreasing the limit in Case 1, the settling time increases to the point that the controller fails to stabilize the system. At odds, in the other case, by decreasing the limit, settling time remains constant, followed by a decrease to a point after which the controller fails to perform the exchange.

In this paper, only the settling time has been used to assess the controller's performance in the presence of the delay and actuator constraints. Employing another criterion will help in investigating the controller's performance. The current criterion indicates the speed at which the controller drives the system to the desired response. However, it does not investigate or illustrate how stable the response is. In other words, it does not indicate how much disturbance the system can tolerate in the settled response before it becomes unstable. Moreover, the underlying physics behind the illustrated patterns requires further investigation. Hence, as future work, stability analysis using Floquet theory [38] is advisable to investigate the underlying dynamics of the delayed system in terms of the leading Floquet branches and its effect on the stability and performance of the controller.

Conflict of interest

On behalf of all authors, the corresponding author states that there is no conflict of interest.

References

[1] Pisarchik, A.N., Feudel, U.: Control of multistability. Physics Reports **540**(4), 167–218 (2014)

[2] Pisarchik, A., Jaimes-Reátegui, R., Villalobos-Salazar, J., Garcia-Lopez, J., Boccaletti, S.: Synchronization of chaotic systems with coexisting attractors. Physical review letters **96**(24), 244102 (2006)

[3] Feudel, U., Kurths, J., Pikovsky, A.S.: Strange non-chaotic attractor in a quasiperiodically forced circle map. Physica D: Nonlinear Phenomena **88**(3-4), 176–186 (1995)

[4] Chiacchiari, S., Romeo, F., McFarland, D.M., Bergman, L.A., Vakakis, A.F.: Vibration energy harvesting from impulsive excitations via a bistable nonlinear attachment. International Journal of Non-Linear Mechanics **94**, 84–97 (2017)

[5] Geltrude, A., Al Naimee, K., Euzzor, S., Meucci, R., Arecchi, F.T., Goswami, B.K.: Feedback control of bursting and multistability in chaotic systems. Communications in Nonlinear Science and Numerical Simulation **17**(7), 3031–3039 (2012)

[6] Guo, B., Liu, Y., Birler, R., Prasad, S.: Self-propelled capsule endoscopy for small-bowel examination: proof-of-concept and model verification. International Journal of Mechanical Sciences **174**, 105506 (2020)

[7] Wiercigroch, M., Krivtsov, A.M.: Frictional chatter in orthogonal metal cutting. Philosophical Transactions of the Royal Society of London. Series A: Mathematical, Physical and Engineering Sciences **359**(1781), 713–738 (2001)

[8] Budd, C., Dux, F.: Chattering and related behaviour in impact oscillators. Philosophical Transactions of the Royal Society of London. Series A: Physical and Engineering Sciences **347**(1683), 365–389 (1994)

[9] Mora, K., Champneys, A.R., Shaw, A.D., Friswell, M.I.: Explanation of the onset of bouncing cycles in isotropic rotor dynamics; a grazing bifurcation analysis. Proceedings of the Royal Society A **476**(2237), 20190549 (2020)

[10] Chávez, J.P., Wiercigroch, M.: Bifurcation analysis of periodic orbits of a non-smooth jeffcott rotor model. Communications in Nonlinear Science and Numerical Simulation **18**(9), 2571–2580 (2013)

[11] Miao, P., Li, D., Yin, S., Xie, J., Grebogi, C., Yue, Y.: Double grazing bifurcations of the non-smooth railway wheelset systems (2021)

[12] Wagg, D., Bishop, S.: Application of non-smooth modelling techniques to the dynamics of a flexible impacting beam. Journal of Sound and Vibration **256**(5), 803–820 (2002)

[13] Liu, R., Yue, Y., Xie, J.: Existence and stability of the periodic orbits induced by grazing bifurcation in a cantilever beam system with single rigid impacting constraint. Communications in Nonlinear Science and Numerical Simulation **121**, 107235 (2023)

[14] Grace, I., Ibrahim, R.: Modelling and analysis of ship roll oscillations interacting with stationary icebergs. Proceedings of the Institution of Mechanical Engineers, Part C: Journal of Mechanical Engineering Science **222**(10), 1873–1884 (2008)

[15] Grace, I., Ibrahim, R.: Vibro-impact interaction of ships with ice. In: ASME Pressure Vessels and Piping Conference, vol. 48272, pp. 433–440 (2008)

[16] Grace, I., Ibrahim, R.: Elastic and inelastic impact interaction of ship roll dynamics with floating ice, pp. 93–104. Springer, Berlin, Heidelberg (2009)

[17] Zhao, X., Dankowicz, H., Reddy, C., Nayfeh, A.: Dynamic simulation of an electrostatically actuated impact microactuator. In: 2004 NSTI Nanotechnology Conference and Trade Show-NSTI Nanotech 2004, pp. 247–250 (2004). Citeseer

[18] Zhao, X., Dankowicz, H., Reddy, C.K., Nayfeh, A.H.: Modeling and simulation methodology for impact microactuators. Journal of Micromechanics and Microengineering **14**(6), 775 (2004)

[19] Wei, S., Hu, H., He, S.: Modeling and experimental investigation of an impact-driven piezoelectric energy harvester from human motion. Smart Materials and Structures **22**(10), 105020 (2013)

[20] Migliniene, I., Ostasevicius, V., Gaidys, R., Dauksevicius, R., Janusas, G., Jurenas, V., Krasauskas, P.: Rational design approach for enhancing higher-mode response of a microcantilever in vibro-impacting mode. Sensors **17**(12), 2884 (2017)

[21] Serdukova, L., Kuske, R., Yurchenko, D.: Post-grazing dynamics of a vibro-impacting energy generator. Journal of Sound and Vibration **492**, 115811 (2021)

[22] Yurchenko, D., Lai, Z., Thomson, G., Val, D.V., Bobryk, R.V.: Parametric study of a novel vibro-impact energy harvesting system with dielectric elastomer. Applied Energy **208**, 456–470 (2017)

[23] Harne, R.L., Wang, K.: A review of the recent research on vibration energy harvesting via bistable systems. Smart materials and structures **22**(2), 023001 (2013)

[24] Pavlovskaia, E., Hendry, D.C., Wiercigroch, M.: Modelling of high frequency vibro-impact drilling. International Journal of Mechanical Sciences **91**, 110–119 (2015)

[25] Li, S., Vaziri, V., Kapitaniak, M., Millett, J.M., Wiercigroch, M.: Application of resonance enhanced drilling to coring. Journal of Petroleum Science and Engineering **188**, 106866 (2020)

[26] Wiercigroch, M., Vaziri, V., Kapitaniak, M.: Red: revolutionary drilling technology for hard rock formations. In: SPE/IADC Drilling Conference and Exhibition (2017). OnePetro

[27] Zhang, Z., Chávez, J.P., Sieber, J., Liu, Y.: Controlling coexisting attractors of a class of non-autonomous dynamical systems. Physica D: Nonlinear Phenomena **431**, 133134 (2022)

[28] Costa, D., Vaziri, V., Pavlovskaia, E., Savi, M.A., Wiercigroch, M.: Switching between periodic orbits in impact oscillator by time-delayed feedback methods. Physica D: Nonlinear Phenomena, 133587 (2022)

[29] Vaziri, V., Kapitaniak, M., Wiercigroch, M.: Suppression of drill-string stick–slip vibration by sliding mode control: Numerical and experimental studies. European Journal of Applied Mathematics **29**(5), 805–825 (2018)

[30] MacLean, J.D., Vaziri, V., Aphale, S.S., Wiercigroch, M.: Suppressing stick–slip oscillations in drill-strings by modified integral resonant control. International Journal of Mechanical Sciences **228**, 107425 (2022)

[31] Araújo, J.M., Santos, T.L.M.: Control of a class of second-order linear vibrating systems with time-delay: Smith predictor approach. Mechanical Systems and Signal Processing **108**, 173–187 (2018)

[32] Dantas, N.J., Dórea, C.E., Araújo, J.M.: Design of rank-one modification feedback controllers for second-order systems with time delay using frequency response methods. Mechanical Systems and Signal Processing **137**, 106404 (2020)

[33] Vaziri, V., Oladunjoye, I.O., Kapitaniak, M., Aphale, S.S., Wiercigroch, M.: Parametric analysis of a sliding-mode controller to suppress drill-string stick-slip vibration. Meccanica **55**(12), 2475–2492 (2020)

[34] Lalehparvar, M., Aphale, S.S., Vaziri, V.: Constrained control of impact oscillator with delay. Mechanisms and Machine Science **125 MMS**, 437–446 (2023)

[35] Wiercigroch, M., Kovacs, S., Zhong, S., Costa, D., Vaziri, V., Kapitaniak, M., Pavlovskaia, E.: Versatile mass excited impact oscillator. Nonlinear Dynamics **99**(1), 323–339 (2020)

[36] Costa, D., Vaziri, V., Kapitaniak, M., Kovacs, S., Pavlovskaia, E., Savi,

M.A., Wiercigroch, M.: Chaos in impact oscillators not in vain: Dynamics of new mass excited oscillator. Nonlinear Dynamics **102**(2), 835–861 (2020)

[37] Pyragas, K.: Continuous control of chaos by self-controlling feedback. Physics letters A **170**(6), 421–428 (1992)

[38] Pyragas, K.: Delayed feedback control of chaos. Philosophical Transactions of the Royal Society A: Mathematical, Physical and Engineering Sciences **364**(1846), 2309–2334 (2006)